Chapter 3

Initial Investigations with Supported Molecular REMP Catalysts

3.0 – Abstract

Successful development of a supported molecular REMP catalyst system was achieved, thereby creating the opportunity to explore its polymerization profiles and topological fidelity for the REMP of cycloolefin monomers. The polymerization profiles of CP, COE, and COD were compared and CP was chosen for subsequent experiments due to its superior processability. Optimization experiments for CP REMP were conducted such that multi-gram quantities of cyclic polycyclopentene could be achieved. Topological fidelity of CP REMP reactions were found to depend on a variety of reaction conditions: monomer purity, choice of solvent, and oxygen contamination. The purity of cyclic polycyclopentene was determined using interaction chromatography.

Chapter 3 Acknowledgments

Bob Grubbs, Scott Virgil

Anthony Ndiripo and Harald Pasch (University of Stellenbosch, South Africa)

3.1 – Introduction

The use of a simple cycloalkene hydrocarbon monomer has been an important aspect of the REMP project since its inception. Unbranched, main-chain polymers lacking heteroatoms were thought to be the best starting point for investigation of the physical properties of melt-state cyclic polymers. Such investigations are more straightforward for simple polymer compositions.[1,2] Additionally, the physical properties of polyethylene (PE) have been thoroughly studied in the literature and would be useful for comparison to the PE derived from our hydrogenated REMP polymers.[1]

The most attractive monomers for initial investigations were cyclopentene (CP), cyclooctene (COE), and cyclooctadiene (COD) due to commercial availability and precedent for their participation in ROMP and REMP reactions. ROMP reactions with CP, COE, and COD were envisioned as a predictor for the polymerization profiles of the more challenging and time-consuming REMP syntheses. These polymers would also constitute a library of linear polymers of varying MW and *Đ* and would provide the linear component in physical blends of ROMP- and REMP-derived polymers of varying composition which could be used in the development of a protocol to quantify the cyclic:linear purity and to establish an analytical detection limit for the same.

A variety of metathesis catalysts were available for exploring the polymerization profiles of low ring strain monomers: the supported molecular REMP catalyst **3.0** and the ROMP catalysts **3.1** – **3.6** (Fig 3.1).

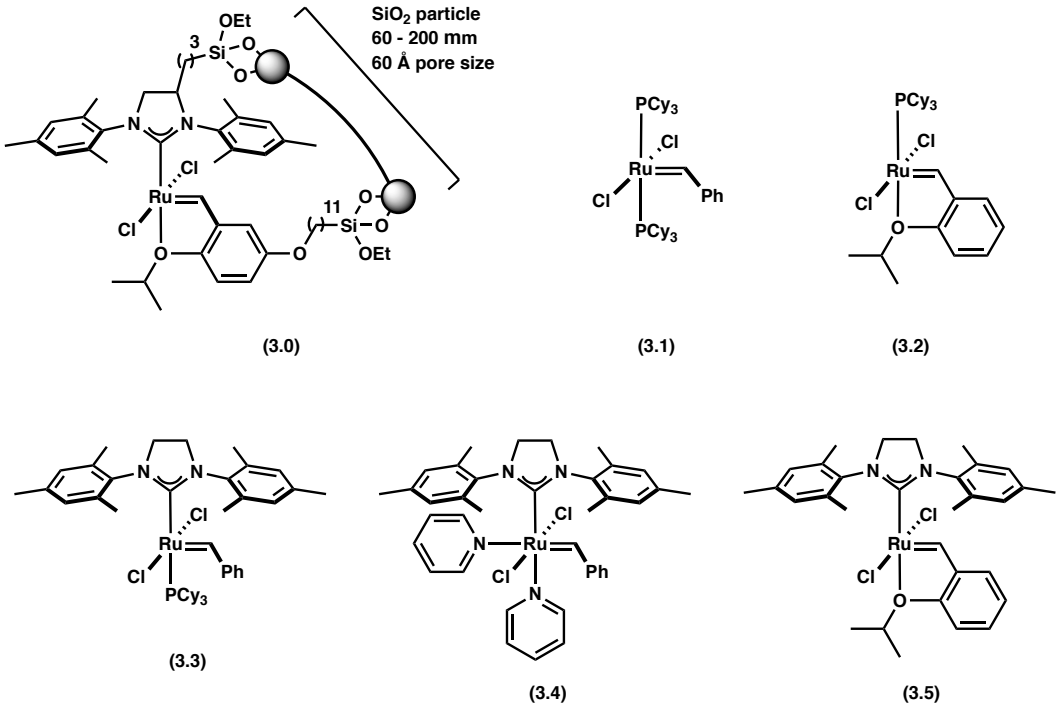

Figure 3.1 | The REMP (**3.0**) and ROMP (**3.1** – **3.5**) catalysts considered for experiment design.

The importance of linear impurity in REMP reactions was reported in our group before the outset of the work described in this chapter.[2] Although a quantitative description of the effects of linear olefin impurity does not exist for REMP, the mechanism by which it was thought to be deleterious was well understood. Every molecule of linear impurity which reacts during REMP (Fig 3.2, red) produces one linear chain. Exclusion of linear olefin impurity and anything which could cause catalyst decomposition was a necessary consideration throughout the design and implementation of the REMP methodology described in this chapter.

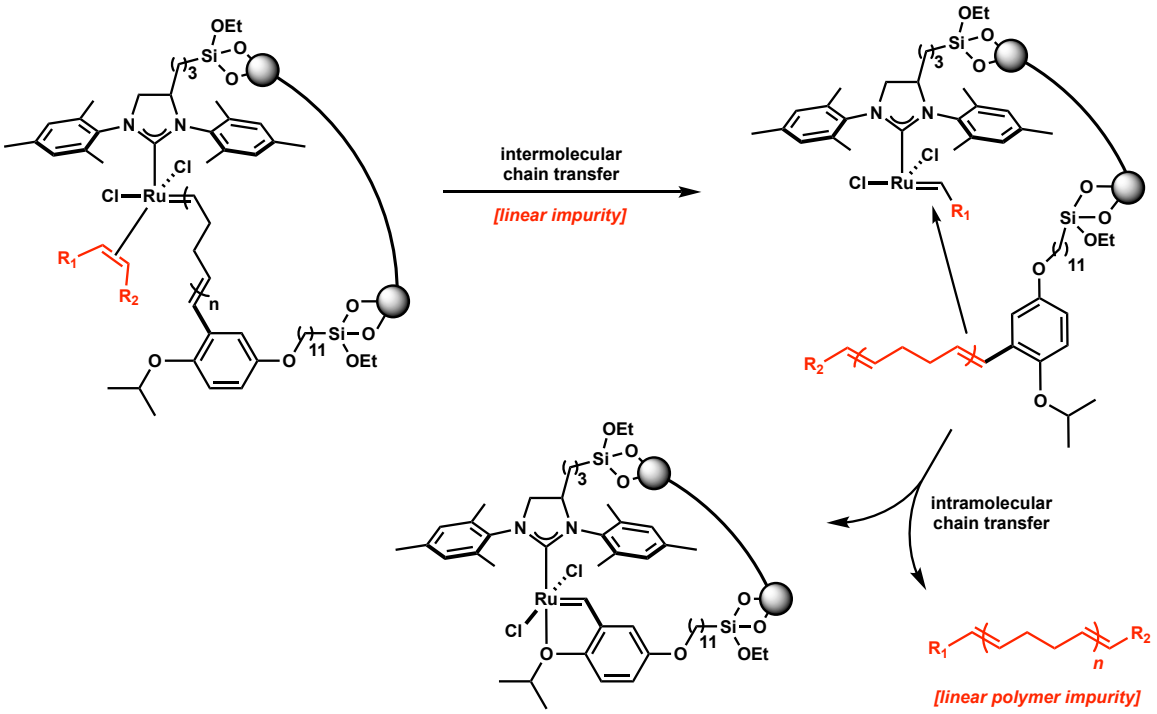

Figure 3.2 | The effect of linear impurity in REMP reactions catalyzed by **3.0**.

3.2 – Results and Discussion

Once a sufficient quantity of catalyst **3.0** was available, an investigation of its polymerization profile and topological selectivity became our primary focus. The supported REMP catalyst **3.0** was used for all cyclic polymers described in this chapter. COE and COD were chosen as the first monomers for exploration of the new catalyst system due to the higher ring strain they possess relative to CP. This ring-strain would provide the enthalpic driving force of polymerization such that higher MW and narrower *Đ* could be achieved.[3] The relative frequency of chain transfer events (secondary metathesis) to monomer propagation (productive metathesis) increases as monomer ring strain decreases. Similarly, at

[monomer]/[polymer] steady-state, low ring strain decreases the frequency of the desired intramolecular chain transfer event which releases a polymer chain, and increases the frequency of undesired monomeric and oligomeric depolymerization events which decrease yield and M_n.

The study of ROMP and REMP profiles of COE and COD was conducted using six individual ruthenium-based metathesis catalysts (Fig 3.1). The development of experimental ROMP procedures and conditions was desired to both serve as a model for REMP reactions with **3.0** (investigation of **3.0** as a polymerization catalyst was unprecedented) and to produce the library of linear polymers for comparison to their cyclic counterparts. To accomplish this, homogeneous catalysts **3.1** – **3.5** were used to provide control of the molecular weight distributions of linear PCOE and PBD due to their distinct initiation and propagation rates (k_i and k_p, respectively). The ratio k_i/k_p is well known to dictate the polymerization characteristics of olefin metathesis catalysts.[4-8]

Initially, COE and COD were successfully polymerized with catalysts **3.1**–**3.5** to high yields (>80%), but were consistently either nearly insoluble or completely insoluble in common organic solvents. This was initially attributed to secondary metathesis reactions leading to abundant chain transfer and thus high M_w and broad $Đ$. Their extremely low solubility in common solvents precluded the acquisition of reliable data. Although the importance of removing impurity from monomer prior to polymerization was known, the extent to which this was

absolutely critical was not initially appreciated. In lieu of problems with COE and COD, ROMP and REMP experiments with CP were then undertaken.

Although initial experiments were somewhat successful, the low M_n and broad dispersity of both linear and cyclic PCP were unacceptably poor. Optimization experiments were begun to improve these properties, but concomitant decomposition of PCP—evident from gradual discoloration and decreasing solubility in common solvents—suggested greater rigor preparing monomer stocks prior to polymerization was necessary.

The lack of instrumentation necessary to determine CP purity necessitated a different approach to assessing purity. An appropriate GC column to separate CP (bp = 44 ºC) was not available. The addition of linear olefin chain transfer agents (CTAs) has been well established to decrease MW by chain-scission via secondary metathesis reactions during ROMP and REMP. [9-11] Therefore, the polymerization of high purity cyclic monomers should give higher M_n polymers. This phenomenon was exploited in a chemical test to indirectly determine the relative purity of 7 successive distillate fractions of CP. Aliquots of each fraction were polymerized in triplicate under identical conditions (Fig 3.3) and the M_n and yields of the resulting PCP measured (Fig 3.4) to determine relative purity. The fractions with the highest M_n were considered to be the most pure. This indirect means to measure relative purity had not been explicitly reported, but it was validated by results to be discussed later in this chapter.

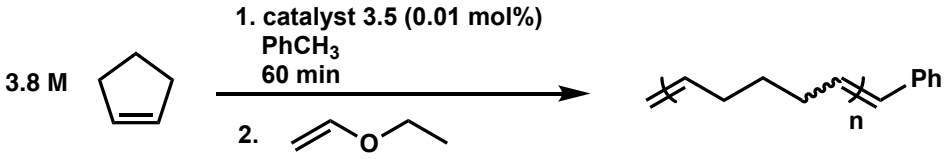

Figure 3.3 | Scheme for the ROMP of 7 successive CP distillate fractions

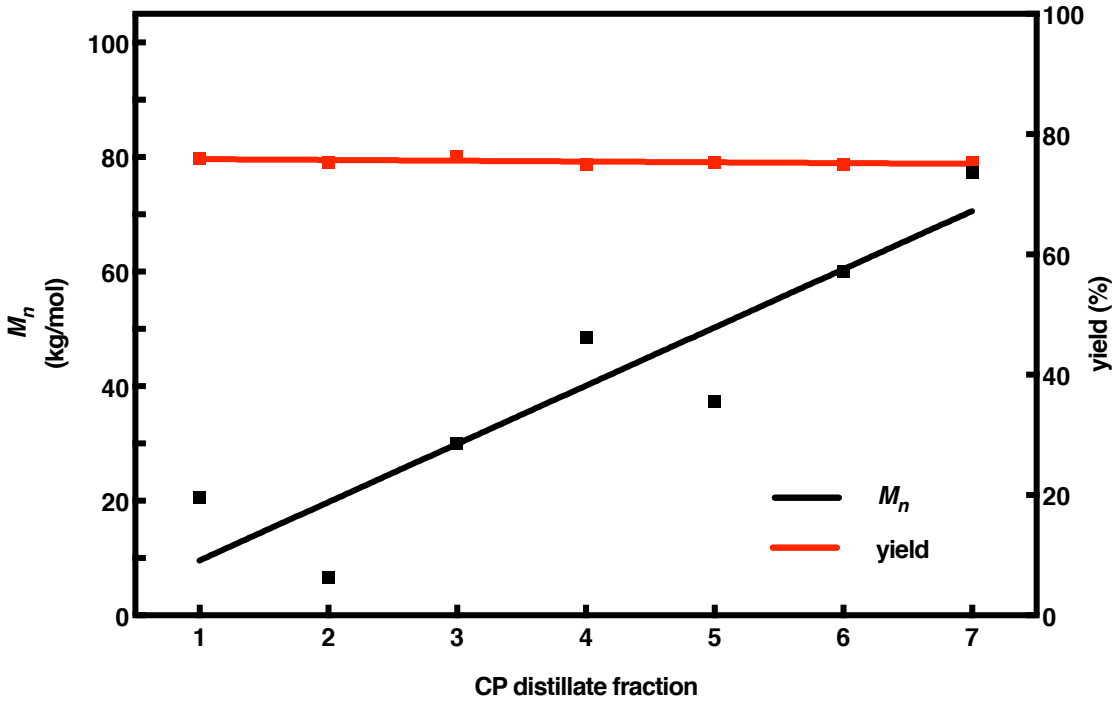

Figure 3.4 | ROMP of 7 successive CP distillate fractions.

The data in Fig 3.4 strongly suggests the presence of CTAs in early CP distillate fractions. The gradual increase in M_n (black line) with the concomitant unchanging yield (red) indicated that the impurity was not inducing catalyst decomposition, which would coincide with reduced yield. Given that ROMP of CP was highly dependent on the purity of the monomer, the rigorous purification of all monomers for both ROMP and REMP was essential.

With the purified CP, we were able to access linear PCP with Mn significantly higher than previously reported examples(Table 3.1).[12-15]

Table 3.1 | The highest MW linear PCPs reported in the literature.

ref.	catalyst loading (ppm)	catalyst	M_n (kg/mol)	$Đ$	time (hr)	yield
Feast et al. (1995)	1700	$Mo[NAr][CHC(CH_3)_2Ph][OCBu^t]_2$	95	1.53	5	-
Register et al. (2000)	100	$W(CHBu^t)(NAr)(OBu^t)_2$	73	1.08	1	-
Register et al. (2008)	330	$Ru(CHPh)(PCy)_3(Cl)_2$	106	1.63	6	-
Register et al. (2017)	400	$Mo[NAr][CHC(CH_3)_2Ph][OCBu^t]_2$	290	1.32	6	<35%

Catalyst **3.5** had previously been chosen for the ROMP of CP because it was the closest analog to supported REMP catalyst **3.0** available. After finding that our CP ROMPs were somewhat controlled when using the pure monomer stock, we investigated the ROMP of CP using **3.1** because it is known to restrict back-biting relative to other ROMP catalysts, despite its low activity. We were able to exceed the highest reported MW of PCP by a factor of 5 (Table 3.2, entry **3.16**).

Table 3.2 | ROMP using the most pure CP monomer stock.

entry	catalyst	catalyst loading (ppm)	M_n (kg/mol)	$Đ$	yield (%)	$[M]_o$ (mol/L)
3.6	3.4	100	116	1.54	52	5.7
3.7	3.4	20	203	1.53	81	5.7
3.8	3.4	10	219	1.51	82	5.7
3.9	3.4	5	205	1.60	82	5.7
3.10	3.4	1	192	1.57	22	5.7
3.11	3.4	0.5	215	1.51	12	11.4
3.12	3.4	5	292	1.48	64	11.4
3.13	3.4	5	258	1.53	87	11.4
3.14	3.4	1	185	1.58	6	11.4
3.15	3.4	5	286	1.46	88	11.4
3.16	3.1	5	1,400	1.42	17	11.4

The ultra-high MW PCP was ultimately unrelated to our goal of producing cyclic polymers via REMP, but we also would not have stumbled across these findings without the extreme rigor in monomer purification for REMP. The ultra-high MW PCP became the subject of ongoing research which will be described later in this dissertation.

A collaboration with the research group of Professor Nikos Hadjichristidis at King Abdullah University of Science and Technology (KAUST) encouraged us to produce the multi-gram quantity of cyclic PCP which would be necessary for his group to perform characterization of its bulk properties. We envisioned a scale-up of CP REMP using catalyst **3.0** would be feasible, and we also sought to determine the feasibility of catalyst **3.0** recycling to produce multiple batches of PCP—this capability was incorporated into our initial catalyst design (Chapter 2), but we had not yet attempted it.

Our large-scale CP REMP succeeded in producing 4 batches of PCP and indicated that low catalyst loading and increased $[CP]_0$ gave higher yields, but control over MW was not achieved (Table 3, **3.17** – **3.20**). During these experiments, PCP was isolated by filtration of the supernatant of the polymerization medium. Solid-supported catalyst **3.0** accumulated on the bottom of the reaction flask and a vertical viscosity gradient was clearly apparent. Filtration was challenging, but nevertheless, we produced quantities sufficient for bulk property analysis.

Table 3.3 | Large-scale catalyst recycling REMP of CP (**3.17** – **3.20**) and REMP viscosity optimization experiments (**3.21** – **3.25**).

entry	solvent	$[CP]_0$:$[3.0]_0$	M_w (kg/mol)	yield (%)	$[CP]_o$ (mol/L)
3.17	$PhCH_3$	48,000	58	70	4.6
3.18	$PhCH_3$	24,000	64	31	2.3
3.19	$PhCH_3$	24,000	62	30	2.3
3.20	$PhCH_3$	10,000	57	56	2.3
3.21	CH_2Cl_2	15,000	44	40	3.3
3.22	4%tBuOH/$PhCH_3$	10,000	55	72	3.3
3.23	4%tBuOH/$PhCH_3$	10,000	58	71	3.3
3.24	1%tBuOH/$PhCH_3$	10,000	55	72	3.3
3.25	$PhCH_3$	10,000	50	43	3.3

We assumed a tractable polymerization medium would yield more PCP with narrower dispersity and better material properties, so we attempted to decrease the viscosity of the polymerization medium by changing solvent conditions. $PhCH_3$ was originally chosen due its low toxicity and reactivity, but CH_2Cl_2 solvated PCP better than any other common solvent. A small-scale REMP

of CP using CH_2Cl_2 was performed (polymer **3.21**) and the filtration was significantly faster (1 minute compared to 45 minutes) because the PCP was well-solvated. Although solvation of the polymerization medium was considerably better with CH_2Cl_2, catalyst **3.0** particles aggregated and were not evenly dispersed, just as with $PhCH_3$.

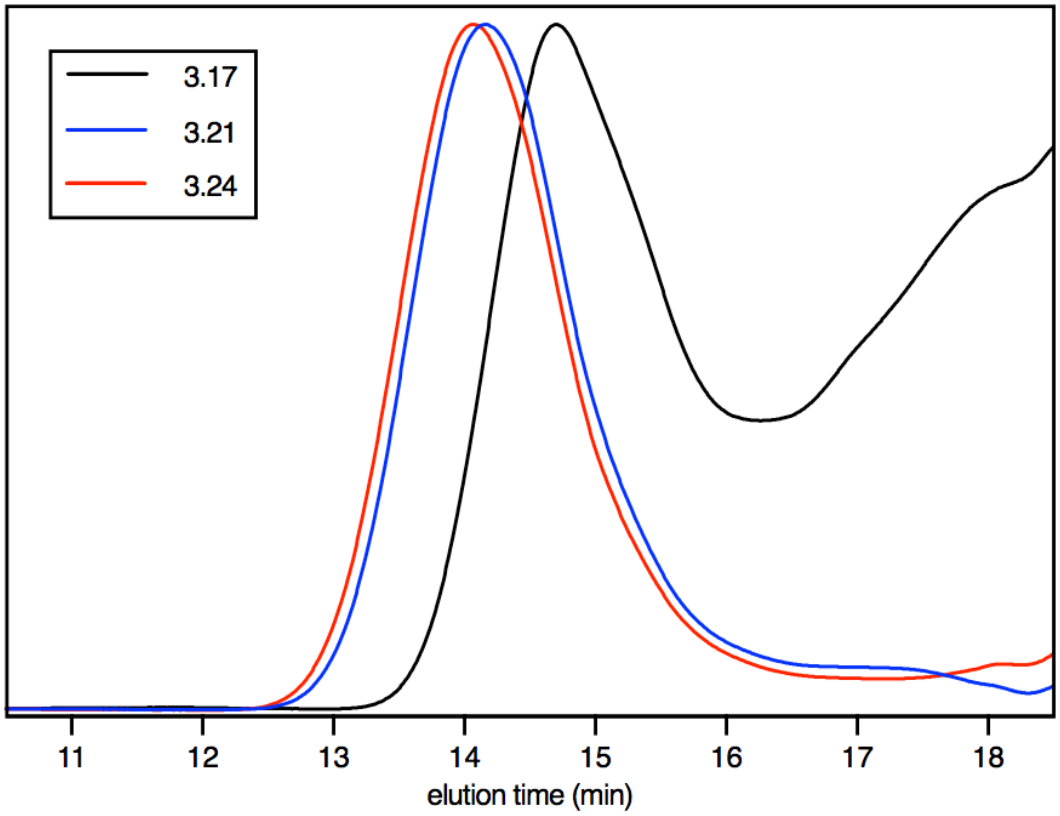

Figure 3.5 | Elution profiles of PCP polymerized in different solvent conditions.

A co-solvent system of $^tBuOH/PhCH_3$ was explored as a means to disrupt the electrostatic forces responsible for catalyst particle aggregation. The $PhCH_3$ would be adequate to solvate the polymer, and a small amount of ^tBuOH would form solvent shells around the catalyst particles through hydrogen bonding with

the SiOH—terminated surface. Visually, the ^{t}BuOH additive had a substantial effect on the polymerization: an evenly dispersed suspension of catalyst particles was immediately apparent and the filtration to isolate the polymer was facile (Table 3.3, polymers **3.22** – **3.24**). Polymers **3.22** – **3.24** were well solvated and gave higher yields than the control, **3.25**. The SEC traces for polymers **3.17** ($PhCH_3$ solvent), polymer **3.21** (CH_2Cl_2 solvent), and polymer **3.24** (^{t}BuOH/$PhCH_3$ cosolvent)(Fig 3.5) clearly indicated that good solvents provide narrow D and higher MW. With this important information in hand, our attention then turned to analysis of PCP topological purity.

All of the PCP samples listed in Table 3.3 were analyzed using an HT-HPLC system operating in interaction chromatography (IC) mode, which separates polymers by composition, as opposed to size-exclusion chromatography (SEC), which separates polymers by hydrodynamic volume. [16-18] Other than the type of separation column used, the key distinction of IC vs. SEC is the use of a solvent gradient. Each cyclic chain has a distinct column condition at which it separates from its linear counterpart of the same MW. By gradually varying the composition of the IC eluent, each cyclic chain can be separated from its linear counterpart. This requires a judicious choice of IC column, solvent system, and temperature. For the work described herein, the solvent gradient changed with the relative ratio of 1-decanol to 1,2,4-trichlorobenzene (Fig 3.6).

The IC chromatograms for **3.17** – **3.25** (Fig 3.7) show that topology depends on both monomer purity and choice of solvent. The linear region in

polymers **3.17** – **3.20** was likely due to impurity in the monomer. They were prepared with the second-most pure CP distillate fraction (Fig 3.3, Fraction 6). The purest fraction only consisted of approximately 10 mL, so it could not be used for large-scale REMP experiments.

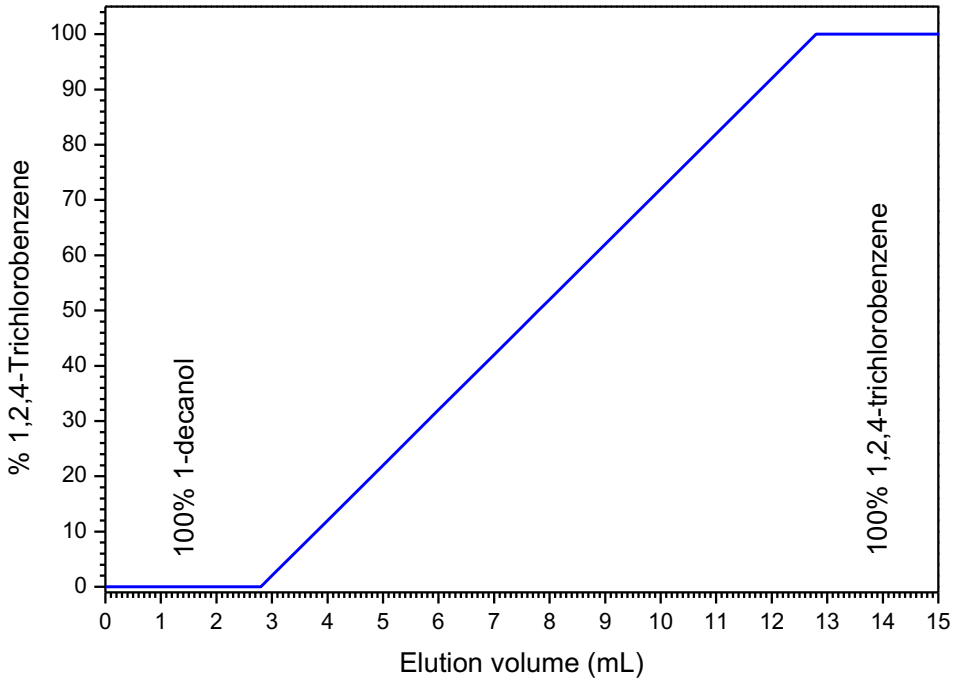

Figure 3.6 | The solvent gradient used in IC for PCP analysis.

The choice of CH_2Cl_2 for **3.21** strongly affected the cyclic purity by IC (Fig 3.5). This may have been due to linear C5 contaminants which were present in the CH_2Cl_2. To prevent carbene formation, CH_2Cl_2 is often stabilized with 150 ppm amylenes (mixture of pentene isomers), which was the case for solvent used in REMP polymer **3.21**. Alternatively, CH_2Cl_2 may have facilitated deleterious catalyst detachment from the SiO_2 particle surface which would produce linear chains. Similarly, the $^tBuOH/PhCH_3$ co-solvent system seemed promising, but the

linear region for **3.22** – **3.24** suggests it leads to considerable linear impurity. A definite explanation for this could not be made, but catalyst detachment caused by ^{t}BuOH may have been the root cause. However, polymer **3.25** appears purely cyclic by IC (Fig 3.7), and polymer **3.24**, produced with only 1% ^{t}BuOH appears nearly as pure. The instrumentation and techniques available at the time precluded direct measurement of cyclic purity by IC, but we learned about the paramount importance of solvent and monomer purity during REMP nonetheless. Although monomer purity was already known to be important, the extent to which it was important was admittedly not fully appreciated at the outset of this work.

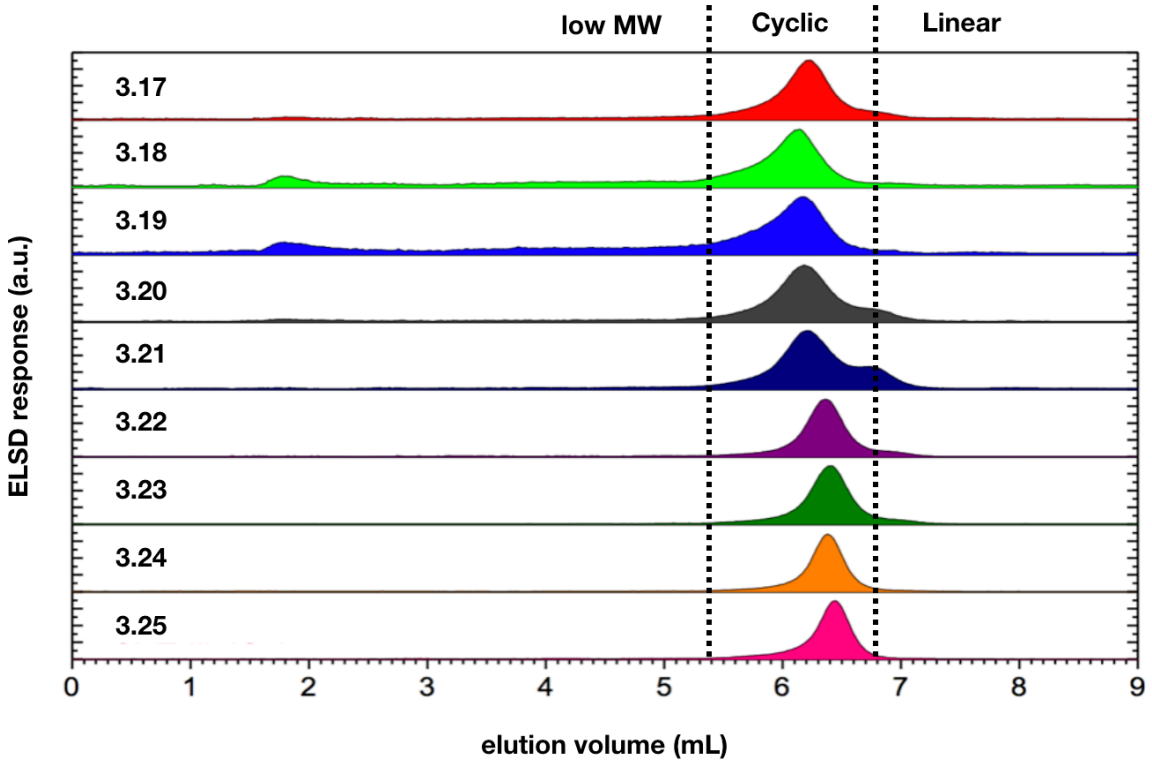

Figure 3.7 | IC of PCPs **3.17** – **3.25** with low MW, cyclic, and linear elution components demarcated by dotted lines.

A 2D IC-SEC elution method was used to ascertain the molecular homogeneity of polymers **3.17** and **3.20** (Fig 3.8). Elution conditions using this technique ideally separate polymers exclusively by either IC or SEC principles. In that case, polymers with topological homogeneity but a distribution of MWs would elute simultaneously in IC (Fig 3.8, y-axis), and be separated only by SEC (Fig 3.8, x-axis). Similarly, polymers with different topologies but identical and monodisperse MWs would elute simultaneously in SEC (Fig 3.8, x-axis), and be separated only by IC (Fig 3.8, y-axis). This ideal case cannot be achieved with modern instrumentation and techniques, but comparisons of the molecular homogeneity can be made based on the topography of the 2D IC-SEC chromatograms. Polymer **3.17** has a more broad and gradually changing evaporative light-scattering detector (ELSD) response than for polymer **3.20** which indicates it is less topologically pure. This can be explained by making an analogy to topographical maps: if **3.17** and **3.20** were mountains, **3.20** would be much steeper than **3.17**; the steeper the "mountain," the more topologically pure it is. We believe **3.17** is less pure topologically than **3.20** because it was produced from REMP catalyst which had been recycled 3 times prior and so levels of adventitious O_2 were likely higher. O_2 would have caused catalyst decomposition which we have long suspected leads to linear polymer impurity.[16]

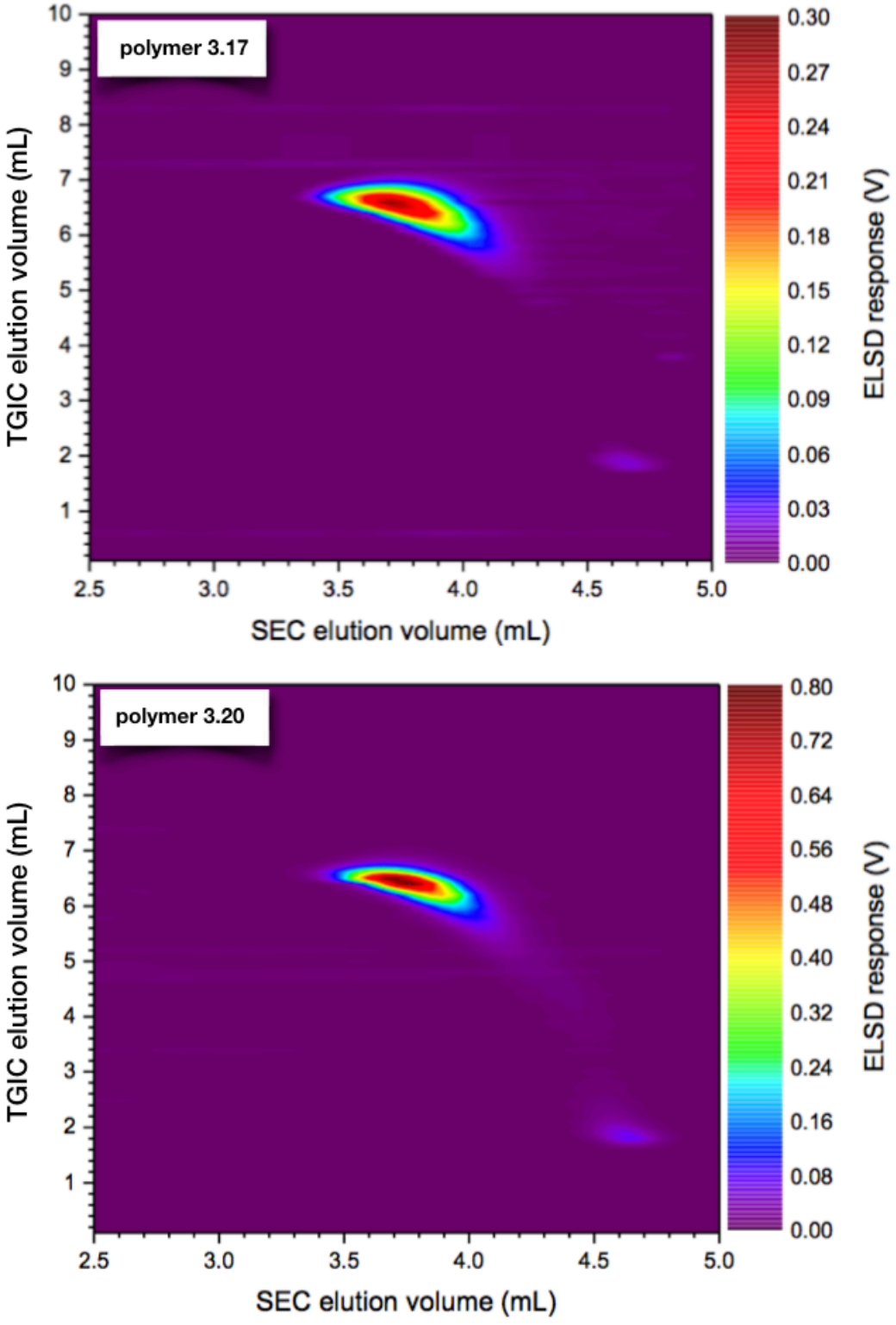

Figure 3.8 | 2D IC-SEC for polymers **3.17** and **3.20**.

3.4 – Conclusion and Future Work

The capabilities of supported molecular REMP catalyst **3.0** were explored. REMP reactions with simple cycloolefin monomers COE, COD, and CP were conducted, which led us to pursue CP as the best REMP monomer due to its superior processability. The purity of CP was found to be critical for ensuring purely cyclic polymer product. Evidence for linear pentene isomers as contaminants in certain CP monomer stocks was found. The topological purity of PCP was confirmed using IC and 2D IC-SEC.

Experimental conditions were successfully determined as the basis for future REMP work. The knowledge and expertise necessary to explore the polymerization profiles and reactivities of other cycloolefin monomers was achieved.

3.4 – Experimental

General Information

All reactions were carried out in glassware flame-dried in vacuo (100 mTorr) unless otherwise specified. Reactions were performed using air-free Schlenk technique (100 mTorr vacuum and UHP grade 5.0 argon gas) on the benchtop or in a Vacuum Atmospheres glovebox (N_2-filled, O_2 concentration < 0.25 ppm) unless otherwise specified. All solvents were purchased from Sigma-Aldrich (anhydrous, 99.9%) and further purified by passage through solvent purification columns, sparged with argon, and then stored over 4 Å molecular sieves in Strauss flasks, unless otherwise specified.[17] All homogeneous Grubbs catalyst

(**3.1** – **3.6**, Fig 3.1) were received as a generous gift by Materia, Inc. (Pasadena, CA) and used without further purification. All other reagents were purchased from Sigma-Aldrich and used as received unless otherwise stated. Room temperature was 18-20 °C for all syntheses described herein.

All ^{1}H NMR spectra were acquired using a Varian Inova 500 MHz or Bruker 400 MHz spectrometer and are reported relative to residual $CHCl_3$ (δ 7.26 ppm), C_6H_6 (δ 7.16 ppm), or CH_2Cl_2 (δ 5.32 ppm). All ^{13}C NMR spectra were recorded on a Varian Inova 500 MHz spectrometer (125 MHz) or Bruker 400 MHz spectrometer (100 MHz) and are reported relative to $CHCl_3$ (δ 77.16 ppm). Data for ^{13}C NMR are reported in terms of chemical shifts (δ ppm). Processing of all NMR data was performed with MestReNova version 10.0 from Mestrelabs Research S.L.

Size-exclusion chromatography (SEC) data was obtained with an HPLC system consisting of two two Agilent PLgel MIXED-B 300×7.5 mm columns with 10 μm beads, and an Agilent 1260 Series pump and autosampler; the columns were connected in series with a Wyatt 18-angle DAWN HELEOS multi-angle laser light scattering detector and Optilab rEX differential refractive index detector. The mobile phase was either pure THF or stabilized THF (50-150 ppm butylated hydroxytoluene (BHT).

Orbital agitation of REMP reactions was performed using an IKA KS 260 basic flat orbital shaker with a swivel motion (no z-axis motion). Orbital agitation rate varied between 200 and 400 rot/min.

Fractional distillation of cyclopentene

The following procedure was adapted from a procedure reported in patent literature.[18] Fractional distillation of cyclopentene was conducted using a 24-inch Pro-Pak® column which was the best performing fractionating column available. Prior to the collection of distillate fractions, the crude cyclopentene was refluxed for 48 hours over 20 weight percent H-form Amberlyst® 15 resin which was reported to effect the acid-catalyzed oligomerization of olefinic impurity. Following this procedure, 7 CP distillate fractions were collected over 48 hours with the distillation pot held at a temperature such that CP distilled slowly, dropwise. Instrumentation to directly measure purity was not available, so an indirect method for purity determination was devised and conducted. The seven distillate fractions collected were stored in Schlenk flasks and degassed by ultra-high purity (UHP) argon sparging prior to use (UHP argon had not previously been used). Each CP distillate fraction was then subjected to identical ROMP conditions in triplicate. The molecular weights and yields were used to measure the relative purity of CP batches (Figure 3.4) because an absolute purity determination was not possible due to instrumental limitations.

Interaction chromatography

IC experiments were performed using a solvent gradient interaction chromatograph (SGIC) constructed by Polymer Char (Valencia, Spain). For solvent gradient elution in HPLC, a high- pressure binary gradient pump (Agilent, Waldbronn, Germany) was utilized. The evaporative light scattering detector

(ELSD, model PL-ELS 1000, Polymer Laboratories, Church Stretton, England) was used with the following parameters: gas flow rate of 1.5 SLM, 160 °C nebuliser temperature and an evaporative temperature of 270 °C. A Hypercarb column (Hypercarb®, Thermo Scientific, Dreieich, Germany) with 100 × 4.6 mm internal diameter packed with porous graphite particles which have a particle diameter of 5 µm (making a surface area of 120 m^2g^{-1}) and pore size of 250 Å was used for all HT-HPLC experiments. The column was placed in an oven and the temperature maintained at 160 °C. The flow rate of the mobile phase during analysis was 0.5 $mLmin^{-1}$. To achieve separation, a linear gradient was applied from 100 % 1-decanol to 100 % TCB within 10 min after sample injection. These conditions were held for 20 minutes before re-establishing 1-decanol to 100 %. For all HT-HPLC analyses a concentration of 1 – 1.2 $mgmL^{-1}$ was used (approximately 4 mg in 4 mL of 1-decanol) with 20 µL of each sample being injected.

2D-IC-SEC

HT-HPLC and HT-SEC were coupled with the aid of an electronically controlled eight-port valve system (VICI Valco instruments, Houston, Texas) equipped with two 100 µL sample loops. Injection into the first dimension (HT-HPLC) was carried out using a 110 µL sample loop and the flow rate was 0.05 $mLmin^{-1}$. A linear gradient was applied from 100% 1-decanol to 100% TCB within 20 mL (200 mins). A flow rate of 2.75 $mLmin^{-1}$ was used in the second

dimension (HT-SEC) and TCB was used as the mobile phase. In the second dimension, a PL Rapide H (Polymer Laboratories, Church Stretton, U.K.) 100 × 10 mm internal diameter column with a 6 μm particle diameter was used at 160 °C. The column was kept in an oven at this temperature during the analysis. The evaporative light scattering detector (ELSD, model PL-ELS 1000, Polymer Laboratories, Church Stretton, England) was used with the following parameters: gas flow rate of 1.5 SLM, 160 °C nebuliser temperature and an evaporative temperature of 270 °C.

Large-scale PCP REMP

A 1.0 L 2-neck round bottom flask was flamed-drie, and charged with 1.20 g catalyst **3.0** (0.024 mmol) in the glovebox. The flask was removed from the glovebox and charged with 104 mL anhydrous $PhCH_3$, followed by 21.1 mL CP (batch 5, figure 3.4). Orbital agitation at 150 rot/min. A separate air-free fritted filtration funnel with round-bottom collection flask was set up nearby, and after 45 minutes, the REMP reaction medium was allowed to settle and the supernatant was cannula transferred (two 18 gauge cannulae) into the filtration apparatus. Following filtration, additional PhCH3 was added to wash the reaction flask, and the supernatant was again transferred into the filtrartion funnel. This process was repeated 4 times (Table 3.4.1). Each cycle was concentrated in vacuo (100 mTorr) for isolation.

Table 3.4.1 | Large-scale CP REMP reaction paramaters.

cycle	volume CP (mL)	volume $PhCH_3$ (mL)	$[CP]_0$ (mol/L)	reaction time (min)	$[CP]_0$:$[cat\ 3.0]_0$
1	21.1	104	2.3 M	45	10000
2	24.0	130	2.3 M	30	11000
3	50	250	2.3 M	25	24000
4	100	250	4.6 M	50	48000

3.5 References

(1) Bielawski, C. W.; Grubbs, R. H. *Science* **2002**, *297* (5589), 2041–2044.
(2) Bielawski, C. W.; Benitez, D.; Grubbs, R. H. *J. Am. Chem. Soc.* **2003**, *125* (28), 8424–8425.
(3) Hejl, A.; Scherman, O. A.; Grubbs, R. H. *Macromolecules* **2005**, *38* (17), 7214–7218.
(4) Grubbs, R. H. *Tetrahedron* **2004**, *60* (34), 7117–7140.
(5) Schwab, P.; France, M. B.; Ziller, J. W.; Grubbs, R. H. *Angew. Chem. Int. Ed.* **1995**, *34* (18), 2039–2041.
(6) Scholl, M.; Ding, S.; Lee, C. W.; Grubbs, R. H. *Org. Lett.* **1999**, *1* (6), 953–956.
(7) Choi, T.-L.; Grubbs, R. H. *Angew. Chem. Int. Ed. Engl.* **2003**, *42* (15), 1743–1746.
(8) Trnka, T. M.; Grubbs, R. H. *Acc. Chem. Res.* **2001**.
(9) Ji, S.; Hoye, T. R.; Macosko, C.; 2004. *Macromolecules* **2004**, *37* (15), 5485–5489.
(10) Morita, T.; Maughon, B. R.; Bielawski, C. W.; Grubbs, R. H. *Macromolecules* **2000**, *33* (17), 6621–6623.
(11) Hillmyer, M. A.; Grubbs, R. H. *Macromolecules* **1995**, *28* (25), 8662–8667.
(12) Dounis, P.; Feast, W. J.; Kenwright, A. M. *Polymer* **1995**, *36* (14), 2787–2796.
(13) Trzaska, S. T.; Lee, L.; Register, R. A. *Macromolecules* **2000**, *33* (25), 9215–9221.
(14) Myers, S. B.; Register, R. A. *Polymer* **2008**, *49* (4), 877–882.
(15) Mulhearn, W. D.; Register, R. A. *ACS Macro Lett.* **2017**, *6* (2), 112–116.
(16) Xia, Y. *California Institute of Technology* **2010**, 1–208.
(17) Pangborn, A. B.; Giardello, M. A.; Grubbs, R. H.; Rosen, R. K.; Timmers, F. J. *Organometallics* **1996**, *15*, 1518–1520.
(18) Johnson, M. M.; Tabler, D. C. US Patent Office 1971.